DOI: 10.1002/ejic.200901116

Double-Shelled Mn_2O_3 Hollow Spheres and Their Application in Water Treatment

Jie Cao,[a] Yongchun Zhu,[a] Liang Shi,[a] Lingling Zhu,[a] Keyan Bao,[a] Shuzhen Liu,[a] and Yitai Qian*[a]

Keywords: Adsorption / Double-shelled structures / Hollow spheres / Manganese / Oxides / Phenol

Double-shelled Mn_2O_3 hollow spheres have been successfully prepared on a large scale by using core-shell-structured $MnCO_3$ microspheres as sacrificial templates. This new method is based on an inward oxidation/etching treatment and sequential heat treatment in air. The as-prepared double-shelled Mn_2O_3 hollow spheres consist of small nanoparticles with a size of ca. 50 nm, and there are many nanopores among the particles. As the double-shelled Mn_2O_3 hollow spheres were employed in water treatment, they could remove about 86 % of phenol without any other additives.

Introduction

Hollow micro- and nanostructures have been greatly explored owing to their potential applications in catalysis, photonic crystals, drug delivery, light filter, waste removal and so on.[1–4] However, in most cases, only single-shelled hollow spheres could be fabricated through template-assisted,[5,6] or template-free methods.[7,8] Recently, double-shelled hollow structures have attracted great attentions because of their promising advantage over their single-shelled counterparts. For example, the shell-in-shell polyelectrolyte capsules exhibit high mechanical stability and preserved permeability.[9] The higher gas sensitivity of double-shelled ferrihydrite hollow spheres is attributed to larger surface areas than those with a single shell.[10] To date, the synthesis of such double-shelled structures is essentially based on using a hard template,[11–13] soft template,[14] an intermediate-templating phase-transformation process,[15] or a twice-gas-bubble template.[10] But the preparation of other materials with such a complex structure without using the shell-by-shell technique remains a great challenge. In particular, the realization of the synthesis of double-shelled hollow spheres by using core-shell structured material as template has been rarely reported.

Mn_2O_3, as a multifunctional material, has been investigated due to its interesting properties and a wide variety of potential applications in waste removal, catalysis, rechargeable batteries, magnetic materials, and so forth.[16,17] Among the applications of waste removal, Mn_2O_3 is known as an inexpensive, environmentally friendly catalyst to remove carbon monoxide and nitrogen oxide from waste gases,[17] which inspired us to use Mn_2O_3 as an adsorbent in water treatment, especially in the treatment of waste water containing highly toxic phenol. In the past decade, great efforts have been devoted to the synthesis of Mn_2O_3 with different morphologies including rods, wires, cubes, octahedral and hollow structures, etc.[18–22] It has been reported that the morphology and dimensions exert a significant influence on the physical and chemical properties of micro- and nanomaterials. Therefore, controlled preparation of Mn_2O_3 with desired morphology, shape, and size may induce novel properties and subsequently better applications. Herein we report the synthesis of Mn_2O_3 hollow spheres with doubled shells constructed by nanocrystals. More importantly, our approach offers an opportunity to investigate the application of Mn_2O_3 in water treatment. The high removal capacity for phenol makes Mn_2O_3 an alternative material for water treatment, thereby extending the application fields of Mn_2O_3.

Results and Discussion

The crystal structure of the as-synthesized product was examined by powder X-ray diffraction (XRD), and the result is shown in Figure 1. All the diffraction peaks correspond to the pure cubic Mn_2O_3 (JCPDS No. 89-4836).

Figure 2 shows scanning electron microscopy (SEM) and transmission electron microscopy (TEM) micrographs of a typical sample. From SEM observations, it can be seen that the as-prepared double-shelled Mn_2O_3 hollow spheres are monodisperse and well defined (image a in Figure 2). The interior space of the product is clearly revealed on the SEM image for a broken sphere (Figure 2b), which indicates the double-shelled architecture in radial direction. Figure 2c

[a] Hefei National Laboratory for Physical Science at Microscale and Department of Chemistry, University of Science and Technology of China,
Hefei, Anhui 230026, People's Republic of China
Fax: +86-551-360-7402
E-mail: ytqian@ustc.edu.cn

Supporting information for this article is available on the WWW under http://dx.doi.org/10.1002/ejic.200901116.

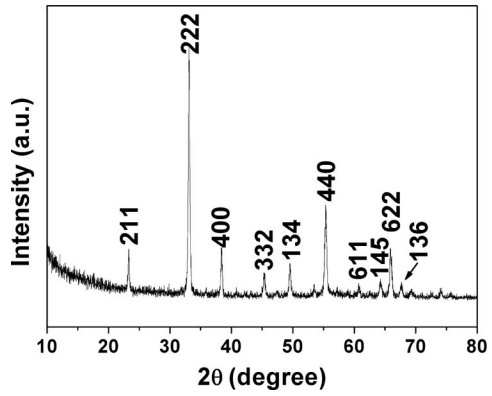

Figure 1. XRD pattern of the as-prepared double-shelled Mn_2O_3 hollow spheres.

shows a low-magnification TEM image displaying double-shelled, concentric Mn_2O_3 hollow spheres in which the diameters of outer spheres and inner spheres are approximately 2.3 and 1.1 μm, respectively. Figure 2d gives the typical TEM image of a representative double-shelled hollow sphere at high magnification. The obvious contrast between the dark solid edges and the pale hollow space confirms the existence of a double-shelled hollow structure in the resulting spheres. The thickness of the inner and outer shells is estimated to be 250 nm, and the distance between the shells is about 230 nm. A more detailed structural information is given in Figure S1, which makes it clear that the Mn_2O_3 shell is composed of nanoparticles with an average size of about 50 nm, and there are many nanopores among the Mn_2O_3 particles.

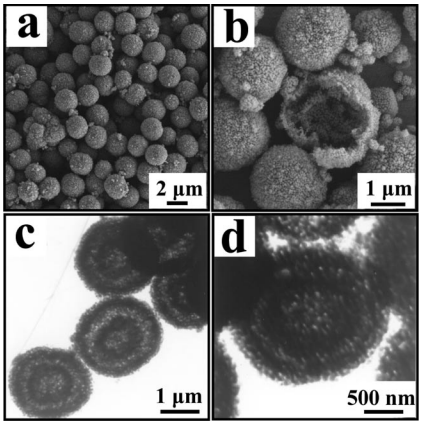

Figure 2. Images of double-shelled Mn_2O_3 hollow spheres: (a) SEM image of the product in a panoramic view; (b) SEM image of a detailed view of a broken double-shelled hollow sphere, showing its hollow interior; (c) TEM image at a low magnification, clearly showing the hollow spheres to be double-shelled; (d) TEM image taken from an individual sphere with slightly higher magnification.

In our approach, the double-shelled Mn_2O_3 hollow spheres originate from an $MnCO_3$ precursor, and the spherical morphology is also maintained during the reaction process. To elucidate the formation mechanism of the double-shelled hollow structure, a thorough understanding of the morphology and structure of the $MnCO_3$ precursor is imperative. Figure S2a shows the X-ray diffraction analysis for the precursor. The XRD pattern revealed diffraction peaks, which are characteristic of the $MnCO_3$ crystal with a rhombohedral structure (JCPDS No. 83-1763). Figure 3a presents a panoramic SEM image of the $MnCO_3$ precursor, which is composed of uniform microspheres with a diameter of about 2.3 μm. An SEM image of the cross section of a single $MnCO_3$ microsphere (Figure 3b) clearly demonstrates that the architecture of the microshpere is built from the outer radial structure and the inner nonradial structure. The outer radial structure grows with radial nanopyramids aligned with their growth axes perpendicular to the surface of the microsphere, and the inner core is constructed by densely packed nanoparticles. The formation of the core-shell structure can be described as follows. In the initial stage of the reaction, massive $MnCO_3$ nuclei spontaneously clustered together to minimize their surface energy, and solid spheres constructed by nanoparticles were formed. With the reaction proceeding, nanopyramids grown on the surface of solid spheres led to the formation of the core-shell structure.[23] The nature of the solid structure of the as-obtained $MnCO_3$ precursor can be further confirmed by the TEM image in Figure 3c. By etching the core-shell-structured $MnCO_3$ microspheres with a small amount of hydrochloric acid, the inner cores were firstly dissolved, and novel porous hollow $MnCO_3$ microspheres composed of aligned nanopyramids as shell were obtained (Figure 3d, e). By further increasing the amount of hydrochloric acid, the outer shell of $MnCO_3$ was also dissolved completely. These results indicate that the inner core was firstly dissolved by hydrochloric acid prior to the shell due to the different sizes of the building units between the core and shell, and an excess degree of acidification could completely consume the entire $MnCO_3$ sphere containing the shell. Hence, keeping the amount of hydrochloric acid in an appropriate range is crucial to the construction of porous hollow $MnCO_3$ microspheres.

Thus, the structure formation of the double-shelled Mn_2O_3 hollow spheres is summarized in Scheme 1. Firstly, a unique core-shell-structured $MnCO_3$ microsphere could be obtained as described in detail in the Experimental Section. Then as-prepared $MnCO_3$ microspheres were well-dispersed in a freshly prepared $KMnO_4$ solution. Since the hollow interior space could be created by the subsequent acid treatment of the interior core through the shell, it follows that the as-formed $MnCO_3$ shell must be highly porous. Thus, the $KMnO_4$ solution was efficiently infiltrated into the porous $MnCO_3$ shells through transverse channels. It has been well documented that $MnCO_3$ can be readily oxidized by $KMnO_4$ to MnO_2;[4] therefore, both $MnCO_3$ shells' exterior and interior surfaces as well as the transverse channels were oxidized to form sandwiched hollow spheres (Figures S2b, S3). After selectively removing the entire $MnCO_3$ middle layer by the residual hydrochloric acid, hollow spheres with double shells were created as indicated by TEM (Figure 3f). The corresponding SEM image of an in-

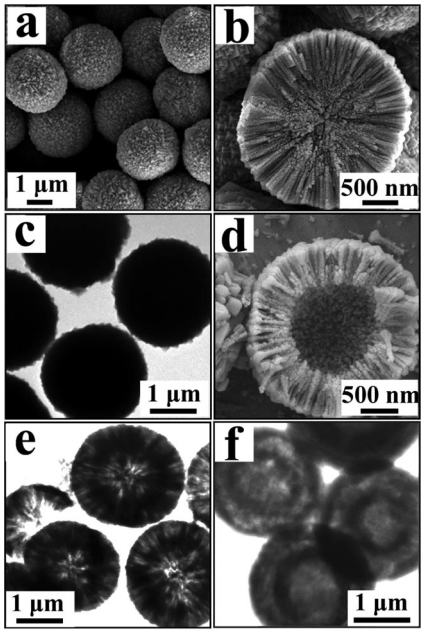

Figure 3. (a) SEM image of the core-shell-structured $MnCO_3$ microsphere; (b) cross-sectional SEM image of a single $MnCO_3$ sphere; (c) TEM image of $MnCO_3$ microspheres; (d, e) SEM and TEM images of porous hollow $MnCO_3$ microspheres, respectively; (f) TEM image of intermediate MnO_2 with double shells.

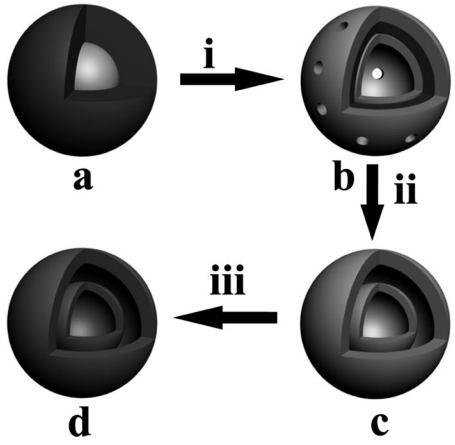

Scheme 1. Schematic illustration of the synthesis of double-shelled Mn_2O_3 hollow spheres: (a) core-shell-structured $MnCO_3$ sphere; (b) sandwiched composite sphere; (c) intermediate MnO_2 with double shells; (d) double-shelled Mn_2O_3 hollow sphere. (i) Acid treatment of the interior core through the shell and $KMnO_4$ oxidation of both its exterior and interior surfaces as well as the transverse channels; (ii) selective removal of the entire $MnCO_3$ middle layer by residual hydrochloric acid; (iii) thermal treatment at 500 °C for 24 h.

complete double-shelled intermediate (Figure S4) demonstrates that the double shells are bridged with pillars, indicating that $KMnO_4$ solution was infiltrated through the porous $MnCO_3$ shell, and oxidation happened not only on the exterior and interior shell surfaces but also within the channels. X-ray photoelectron spectroscopy has been used in the characterization of such a double-shelled intermediate to reveal its phase information. The Mn 2p XPS spectrum (Figure S5) shows two main peaks with band energies at 642 and 654 eV, corresponding to Mn $2p_{3/2}$ and Mn $2p_{1/2}$, respectively, characteristic of an MnO_2 phase. In addition, the XRD result (Figure S2c) shows that the intermediate is poorly crystallized MnO_2, in agreement with the previous report.[24] The intermediate MnO_2 is then converted to Mn_2O_3 by a subsequent calcination in air, while the double-shelled structure remains.

Transition metal oxides are commonly used as adsorbents or catalysts for removal of organic waste from water by adsorption and subsequent catalytic combustion at relatively low temperature.[25,26] Herein, using the prepared double-shelled Mn_2O_3 hollow spheres as adsorbent, we investigated their application in water treatment. Phenol, which is found in industrial effluents such as those generated by petroleum refining and the manufacture of plastics, textile, steel and paper, was chosen as the organic contaminant in the wastewater. Because the high level of toxicity of phenols is considered as primary pollutant in water resources, to eliminate them (by using FePt@C as adsorbent)[27] and develop novel low-cost adsorbents have become important issues.

UV/Vis absorption spectroscopy was applied to record the adsorption behavior of the solution before and after treatment by double-shelled Mn_2O_3 hollow spheres (Figure 4a, b). The characteristic absorption of phenol at 270 nm was chosen for monitoring the adsorption process. The double-shelled Mn_2O_3 hollow spheres prepared here exhibited excellent adsorption capabilities for phenol. For example, 20 mL of phenol solution (100 mg L^{-1}) was mixed with 0.03 g of Mn_2O_3 product, and the mixture was maintained for 300 min whilst stirring; the as-prepared double-shelled Mn_2O_3 hollow spheres could remove most of the phenol at room temperature as shown by the UV/Vis absorption spectra in Figure 4b, with a removal capacity of 86% of phenol without any other additives. The electrostatic attraction between the Mn_2O_3 surface and the phenol species in solution was responsible for the waste removal.[25] Furthermore, the Mn_2O_3 containing phenol could be recycled by a simple thermal treatment in air at 300 °C for 3 h, and the regenerated Mn_2O_3 material kept almost the same adsorption performance as shown in Figure 4c. For comparison, the phenol adsorption property of commercial Mn_2O_3 was also investigated under similar conditions, and it was found that the as-prepared Mn_2O_3 with double-shelled structure showed much better removal capacity than the commercial Mn_2O_3 particles (inset of Figure 4). The better performance might be in relation with an increase in BET surface area, as well as the porous structure. Figure S6 shows the nitrogen adsorption/desorption isotherms and the corresponding pore size distributions of double-shelled Mn_2O_3 hollow spheres and commercial Mn_2O_3. The measurements show that the BET surface area of double-shelled Mn_2O_3 hollow spheres is about 16.3 $m^2 g^{-1}$, which is larger than that of commercial Mn_2O_3 (3.9 $m^2 g^{-1}$). The mean pore diameters of double-shelled Mn_2O_3 and commercial

Mn_2O_3 are 50 and 30 nm, respectively. As the size of the double-shelled Mn_2O_3 is several micrometers, the solid/liquid separation would be fairly easy, which is beneficial for practical application to cut separation costs.

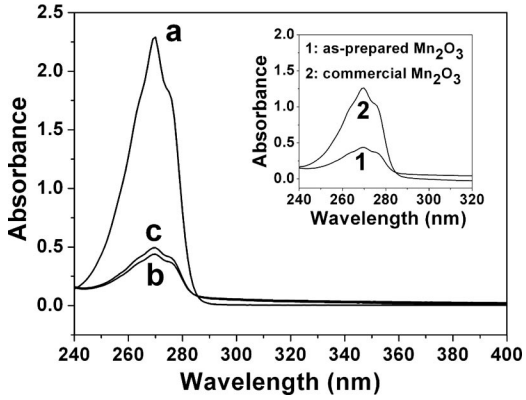

Figure 4. UV/Vis absorption spectra of phenol. Curve (a) corresponds to the spectrum of phenol without adsorption by Mn_2O_3; curves (b) and (c) correspond to the spectra of phenol after treatment with new as-prepared Mn_2O_3 and regenerated Mn_2O_3, respectively. The inset shows the spectra of phenol after adsorption by as-prepared Mn_2O_3 (1), and commercial Mn_2O_3 (2).

Conclusions

We have developed a new route to prepare double-shelled hollow spheres from a core-shell-structured template. It has been found that the formation of porous $MnCO_3$ shells and oxidation of their exterior and interior surfaces as well as the transverse channels by $KMnO_4$ play the key roles in the formation of such double-shelled Mn_2O_3 hollow spheres. The double-shelled Mn_2O_3 hollow spheres prepared here exhibited excellent performance of removing phenol in wastewater, which offers a potential application in water treatment. Furthermore, this synthesis approach may be extended to prepare other oxide systems with such complex structures for other applications.

Experimental Section

General: All the reagents were purchased form Shanghai Chemical Company and used without further purification.

Mn_2O_3 Preparation: In a typical procedure, a manganese sulfate solution (70 mL, 0.014 M) was mixed with ethanol (7 mL) under vigorous stirring. After its complete dispersion, 0.143 M aqueous solution of sodium hydrogen carbonate (70 mL) was added to this mixture. After the resulting mixture was maintained at about 30 °C for 1 h, the $MnCO_3$ microspheres obtained were washed with deionized water and ethanol several times and then dried under vacuum at 60 °C. To obtain double-shelled Mn_2O_3 hollow spheres, the prepared $MnCO_3$ microspheres (0.1 g) were placed in 20 mL of distilled water at room temperature to form a mixed solution by constant stirring. A $KMnO_4$ solution (10 mL, 0.032 M) was then added to the solution, which was continually stirred for 2 min. Then a HCl solution (10 mL, 0.6 M) was directly added to the above solution, and the resulting mixture was maintained for 1 min whilst stirring. The acid-treated product was washed with distilled water and ethanol several times. Next, the product was calcined in an electronic furnace at 500 °C for 24 h in air.

Characterization: The products were characterized by X-ray diffraction (XRD) by using a Japanese Rigaku D/max-γA rotating-anode X-ray diffractometer equipped with monochromatic high-intensity Cu-K_α radiation (λ = 1.54178 Å). The scanning electron microscopy (SEM) images were taken by using a JEOL-JSM-6700F field-emitting (FE) scanning electron microscope. The morphology and structure of the samples were studied with transmission electron microscopy (Hitachi model H-800 instrument and JEOL-2010 TEM) with an accelerating voltage of 200 kV. The X-ray photoelectron spectra (XPS) were collected with an ESCALab MKII X-ray photoelectron spectrometer by using nonmonochromatized Mg-K_α radiation as the excitation source. The Brunauer–Emmett–Teller (BET) surface areas were measured with a Micromeritics ASAP-2020 accelerated surface area and porosimetry system. A TU-1901 UV/Vis spectrometer was used to measure the phenol concentration remaining in the solution.

Supporting Information (see footnote on the first page of this article): TEM and SEM images of the surface of double-shelled Mn_2O_3 hollow spheres; XRD patterns of the as-prepared $MnCO_3$ precursor, sandwiched hollow spheres, and double-shelled MnO_2 hollow spheres; TEM image of the sandwiched hollow spheres; SEM image of a broken double-shelled MnO_2 hollow sphere; XPS spectrum for Mn 2p peaks of double-shelled MnO_2 hollow spheres; nitrogen adsorption/desorption isotherms and the corresponding pore size distributions of double-shelled Mn_2O_3 hollow spheres and commercial Mn_2O_3.

Acknowledgments

Financial support of this work through the 973 Project of China (No. 2005CB623601), is gratefully acknowledged.

[1] F. Caruso, *Chem. Eur. J.* **2000**, *6*, 413–419.
[2] A. D. Dinsmore, M. F. Hsu, M. G. Nikolaides, M. Marquez, A. R. Bausch, D. A. Weitz, *Science* **2002**, *298*, 1006–1009.
[3] L. N. Ye, C. Z. Wu, W. Guo, Y. Xie, *Chem. Commun.* **2006**, 4738–4740.
[4] J. B. Fei, Y. Cui, X. H. Yan, W. Qi, Y. Yang, K. W. Wang, Q. He, J. B. Li, *Adv. Mater.* **2008**, *20*, 452–456.
[5] Z. X. Wang, M. Chen, L. M. Wu, *Chem. Mater.* **2008**, *20*, 3251–3253.
[6] R. M. Garcia, Y. J. Song, R. M. Dorin, H. R. Wang, P. Li, Y. Qiu, F. V. Swol, J. A. Shelnutt, *Chem. Commun.* **2008**, 2535–2537.
[7] X. L. Zhang, R. Qiao, J. C. Kim, Y. S. Kang, *Cryst. Growth Des.* **2008**, *8*, 2609–2613.
[8] T. Nakashima, N. Kimizuka, *J. Am. Chem. Soc.* **2003**, *125*, 6386–6387.
[9] Z. F. Dai, H. Möhwald, B. Tiersch, L. Dähne, *Langmuir* **2002**, *18*, 9533–9538.
[10] Z. C. Wu, M. Zhang, K. Yu, S. D. Zhang, Y. Xie, *Chem. Eur. J.* **2008**, *14*, 5346–5352.
[11] a) X. W. Lou, C. L. Yuan, L. A. Archer, *Adv. Mater.* **2007**, *19*, 3328–3332; b) X. W. Lou, C. L. Yuan, L. A. Archer, *Small* **2007**, *3*, 261–265; c) X. W. Lou, D. Deng, J. Y. Lee, L. A. Archer, *Chem. Mater.* **2008**, *20*, 6562–6566.
[12] a) M. Yang, J. Ma, Z. W. Niu, X. Dong, H. F. Xu, Z. K. Meng, Z. G. Jin, Y. F. Lu, Z. B. Hu, Z. Z. Yang, *Adv. Funct. Mater.* **2005**, *15*, 1523–1528; b) M. Yang, J. Ma, C. L. Zhang, Z. Z. Yang, Y. F. Lu, *Angew. Chem. Int. Ed.* **2005**, *44*, 6727–6730.

[13] a) W. X. Zhang, Z. X. Chen, Z. H. Yang, *Phys. Chem. Chem. Phys.* **2009**, *11*, 6263–6268; b) C. Z. Wu, X. D. Zhang, B. Ning, J. L. Yang, Y. Xie, *Inorg. Chem.* **2009**, *48*, 6044–6054.
[14] H. L. Xu, W. Z. Wang, *Angew. Chem. Int. Ed.* **2007**, *46*, 1489–1492.
[15] H. G. Zhang, Q. S. Zhu, Y. Zhang, Y. Wang, L. Zhao, B. Yu, *Adv. Funct. Mater.* **2007**, *17*, 2766–2771.
[16] a) F. Jiao, J. L. Bao, A. H. Hill, P. G. Bruce, *Angew. Chem. Int. Ed.* **2008**, *47*, 1–7; b) F. Jiao, A. Harrison, A. H. Hill, P. G. Bruce, *Adv. Mater.* **2007**, *19*, 4063–4066.
[17] S. Imamura, M. Shono, N. Okamoto, A. Hamada, S. Ishida, *Appl. Catal. A* **1996**, *142*, 279–288.
[18] Y. C. Chen, Y. G. Zhang, Q. Z. Yao, G. T. Zhou, S. Q. Fu, H. Fan, *J. Solid State Chem.* **2007**, *180*, 1218–1223.
[19] Z. Y. Yuan, Z. L. Zhang, G. H. Du, T. Z. Ren, B. L. Su, *Chem. Phys. Lett.* **2003**, *378*, 349–353.
[20] S. J. Lei, K. B. Tang, Z. Fang, Q. C. Liu, H. G. Zheng, *Mater. Lett.* **2006**, *60*, 53–56.
[21] W. N. Li, L. C. Zhang, S. Sithambaram, J. K. Yuan, X. F. Shen, M. Aindow, S. L. Suib, *J. Phys. Chem. C* **2007**, *111*, 14694–14697.
[22] a) L. Z. Wang, Y. Ebina, K. Takada, T. Sasaki, *Chem. Commun.* **2004**, 1074–1075; b) L. Z. Wang, F. Q. Tang, K. Ozawa, Z. G. Chen, A. Mukherj, Y. C. Zhu, J. Zou, H. M. Cheng, G. Q. Lu, *Angew. Chem. Int. Ed.* **2009**, *48*, 7048–7051; c) J. Cao, Y. C. Zhu, K. Y. Bao, L. Shi, S. Z. Liu, Y. T. Qian, *J. Phys. Chem. C* **2009**, *113*, 17755–17760.
[23] a) W. S. Dong, M. Y. Li, C. L. Liu, F. Q. Lin, Z. T. Liu, *J. Colloid Interface Sci.* **2008**, *319*, 115–122; b) M. Y. Guan, J. H. Sun, M. Han, Z. Xu, F. F. Tao, G. Yin, X. W. Wei, J. M. Zhu, X. Q. Jiang, *Nanotechnology* **2007**, *18*, 415602–415607.
[24] a) X. K. Huang, D. P. Lv, H. J. Yue, A. Attia, Y. Yang, *Nanotechnology* **2008**, *19*, 225606–225612; b) R. N. Reddy, R. G. Reddy, *J. Power Sources* **2004**, *132*, 315–320; c) J. P. Ni, W. C. Lu, L. M. Zhang, B. H. Yue, X. F. Shang, Y. Lv, *J. Phys. Chem. C* **2009**, *113*, 54–60; d) P. Ragupathy, D. H. Park, G. Campet, H. N. Vasan, S. J. Hwang, J. H. Choy, N. Munichandraiah, *J. Phys. Chem. C* **2009**, *113*, 6303–6309.
[25] a) H. M. Chen, J. H. He, *J. Phys. Chem. C* **2008**, *112*, 17540–17545; b) L. S. Zhong, J. S. Hu, H. P. Liang, A. M. Cao, W. G. Song, L. J. Wan, *Adv. Mater.* **2006**, *18*, 2426–2431.
[26] a) Y. M. Zhai, J. F. Zhai, M. Zhou, S. J. Dong, *J. Mater. Chem.* **2009**, *19*, 7030–7035; b) C. C. Yu, X. P. Dong, L. M. Guo, J. T. Li, F. Qin, L. X. Zhang, J. L. Shi, D. S. Yan, *J. Phys. Chem. C* **2008**, *112*, 13378–13382; c) S. W. Cao, Y. J. Zhu, *J. Phys. Chem. C* **2008**, *112*, 6253–6257; d) D. F. Zhang, H. Zhang, L. Guo, K. Zheng, X. D. Han, Z. Zhang, *J. Mater. Chem.* **2009**, *19*, 5220–5225.
[27] Y. F. Zhu, E. Kockrick, S. Kaskel, T. Ikoma, N. Hanagata, *J. Phys. Chem. C* **2009**, *113*, 5998–6002.

Received: November 18, 2009
Published Online: February 8, 2010

